

## Finite Element Analysis of Composite Hardened Walls Subjected to Blast Loads

Girum S. Urgessa

Department of Civil, Environmental and Infrastructure Engineering,  
George Mason University, 4400 University Drive-Mail Stop 6C1, Fairfax, VA 22030

---

**Abstract: Problem statement:** There is currently no standard design guideline to determine the number of composites needed to retrofit masonry walls in order to withstand a given explosion. Past design approaches were mainly based on simplified single-degree-of-freedom analysis. A finite element analysis was conducted for concrete masonry walls hardened with composites and subjected to short duration blast loads. **Approach:** The analysis focused on displacement time history responses which form the basis for retrofit design guidelines against blast loadings. The blast was determined from 0.5 kg equivalent TNT explosive at 1.83 m stand-off distance to simulate small mailroom bombs. Two and four layered retrofitted walls were investigated. Uncertainties in the finite model analysis of walls such as pressure distributions, effect of mid height explosive bursts versus near the ground explosive bursts and variations in modulus of elasticity of the wall were presented. **Results:** Uniformly distributed blast loads over the retrofitted wall height produced a small difference in peak displacement results when compared to the non-uniform pressure distribution. Ground explosive burst was shown to produce a 62.7% increase in energy and a higher peak displacement response when compared to mid-height explosive burst. **Conclusion:** The parametric study on the variation of modulus of elasticity of concrete masonry showed no significant effect on peak displacement affirming the use of the resistance deflection contribution of the composite in retrofit designs.

**Key words:** Finite element analysis, concrete masonry units, composite materials, blast, explosives

---

### INTRODUCTION

Hardening (commonly referred as retrofitting) of a concrete masonry wall can be achieved by producing a field made composite material in an epoxy matrix bonded to the entire surface of the wall. The composite enhances the out-of-plane bending strength of the wall and prevents broken pieces of the wall from entering protected space in an explosion event<sup>[14]</sup>.

Research efforts to develop retrofit design guidelines for structures hardened with composite materials and subjected to blast are mainly based on displacement-time history results obtained from a Single-Degree-Of-Freedom (SDOF) analysis. The shortcoming of the SDOF analysis is that the anticipated mode of response has to be postulated beforehand<sup>[9]</sup>. In addition, SDOF methods are upper bound solutions which provide good insight into peak responses but result in an over-assessment of the complete displacement-time history according to the Rayleigh-Ritz energy principle<sup>[8]</sup>.

Explicit finite element analysis can provide improved displacement-time history predictions and allow investigation of parametric variations that could affect peak displacement results. However, finite element modeling of concrete masonry walls subjected to a blast

load requires a highly non-linear and large displacement approach that allows arbitrary element contact and separation<sup>[7]</sup>. Computationally efficient models are relatively difficult to execute because of uncertainties in blast loads and material properties at high loading rates<sup>[6]</sup>. The explicit dynamic analysis also requires vast computing resources<sup>[1]</sup>. This study presents displacement-time history results obtained from a finite element analysis of a concrete masonry wall retrofitted with different number of composites. The analysis also presented changes in blast response of hardened walls due to assumptions in explosive shape, pressure distribution and modulus of elasticity of the concrete masonry. Currently, there is no design guideline in open literature that allows a designer to specify a number of composites to withstand a quantifiable explosion based on engineering principles. The results of this finite element analysis will supplement the research effort of developing design guidance of composites for blast protection.

### MATERIALS AND METHODS

**Finite element model:** A structure with infinite degrees-of-freedom can be effectively represented by a

discrete system with finite number of degrees-of-freedom. In the finite element scheme, the discrete systems only interact at nodal connectivity. By solving the system of equations of motions for the discrete system, displacements at nodal points are determined. Strains are calculated from nodal displacements and stresses (or pressures) are determined through constitutive laws. Forces will then be derived from the calculated stresses and element volumes. For variables other than nodes, results can be interpolated using interpolation functions that are selected appropriately to form a complete solution. The equation of motion obtained from the principle of virtual work for a single element volume,  $v$  is shown in Eq.1:

$$\int \{\delta u\}^T \{F\} dv + \sum_i^n \{\delta u\}_i^T \{p\}_i = \int [ \{\delta u\}^T \rho \{\ddot{u}\} + \{\delta \epsilon\}^T \{\sigma\} ] dv \quad (1)$$

Where:

- $\{F\}$  = Represents prescribed body forces
- $\{p\}_i$  and  $\{\delta u\}_i$  = Represent prescribed concentrated loads and their corresponding virtual displacements
- $\rho$  = Represents mass density
- $\{\delta \epsilon\}$  = Represents virtual strains
- $\{\sigma\}$  = Denotes internal stresses

In customary notation, the displacement fields  $\{u\}$  and nodal displacements,  $\{d\}$  are related through interpolation functions,  $[N]$  as shown in Eq. 2:

$$\{u\} = [N]\{d\} \quad (2)$$

The strain-displacement relations can be invoked using the  $[B]$  matrix as shown in Eq. 3:

$$\{\epsilon\} = [B]\{d\} \quad (3)$$

Noting that  $[N]$  is a function of space while  $\{d\}$  is a function of time, the work balance can be expressed in the form of Eq.4:

$$[m]\{\ddot{d}\} + \{r\}^{int} = \{r\}^{ext} \quad (4)$$

The above equation indicates that external loads are resisted, dynamically equilibrated by a combination of inertial forces and internal stresses. The equation constitutes a semi-discretization; nodal degrees-of-freedom are discrete functions of space but continuous functions of time.

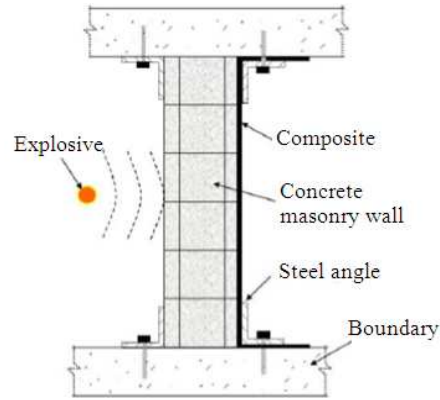


Fig. 1: Concrete masonry wall hardened with composite

Table 1: Composite material properties

Tensile strength	3.8 GPa (575 ksi)
Tensile modulus	242 GPa (35000 ksi)
Elongation	1.5%
Density	1.81 g cm <sup>-3</sup> (0.065 lbs in <sup>-3</sup> )

Discretization in time is accomplished by using finite difference approximations of time derivatives. Methods of direct integration calculate conditions at time step  $i+1$  from the equation of motion, a difference expression and known conditions at one or more preceding time steps. One must choose between an explicit integration method, with low cost per time step with many required steps and an implicit integration method, with higher cost per time step with fewer required steps<sup>[5]</sup>. Explicit integration methods were shown to be best suited for wave propagation problems such as blast and impact loading<sup>[15]</sup>.

**Modeling detail:** A concrete masonry wall, 1.02 m (3.33 ft) wide×3.05 m (10 ft) high×0.2 m (8 in) thick, hardened with uni-directional composites was shown in Fig. 1. The material properties of the unidirectional composites were shown in Table 1. An angle iron connection system was used for anchoring the composite to the surrounding floor and roof boundary. The floor anchorage was consisted of angles (L 6×5½×1/2) whereas the roof anchorage was consisted of lighter angles (L 4×4×3/8). The walls were subjected to an equivalent TNT value of 0.64 kg (1.4 lb) explosive charge at a stand-off distance of 1.83 m (6 ft) for pressure calculations based on the recommendation of the Structural Engineering Institute for small mailroom bombs<sup>[4]</sup>.

The finite element analysis software used to model the wall is NLFlex<sup>[13]</sup>. The program performs transient dynamic analyses using an explicit time integration technique that require small time steps for computation

and to satisfy dynamic courant stability criteria. The program also contains a library of finite elements and constitutive models that are tailored to the solution of large, transient and non-linear problems<sup>[11]</sup>.

The basic element used in the model was an 8-noded hexahedral iso-parametric element. The iso-parametric element utilize the same shape functions relating nodal displacements of a point and nodal coordinates defining global position of a point within an element. Belytschko *et al.*<sup>[3]</sup> has formulated a complete mathematical derivation of shape functions for 8-noded hexahedral iso-parametric elements suited for coding algorithms. The discrete representation of the continuous mass distribution was achieved through the use of lumped mass matrix by placing particle masses at nodes. The advantage of lumping masses at nodes was the reduced computational effort resulting in reduced processing time.

The model grid was built in a text file by combining 0.19 m (7 $\frac{5}{8}$  in) half and 0.40 m full (15 $\frac{5}{8}$  in) concrete masonry units that were 0.40 m (7 $\frac{5}{8}$  in) in depth. The arrangement of one course of the wall cross-section was shown in Fig. 2. Since the walls were 15 courses high with alternating running bonds, two mathematical schemes were developed to generate every even and odd grid of the concrete masonry unit. Two element grids were run on the webs of the concrete masonry unit for better representation of force and displacement results. Similar procedures were implemented for the mortar which is binding the masonry courses. Finally, the supporting structures (the roof and floor), the composite material and the connecting angle grids were generated.

The finite element program did not have a geometry generator for specifying nodal and element coordinates. Hence, the model was built on a uniform ijk space grid which was then mapped to physical xyz space. The supporting roof and floor were modeled on a separate ijk space and later connected to the walls in physical xyz space. All material properties, regeneration of elements, boundary conditions and loadings were assigned in a separate file.

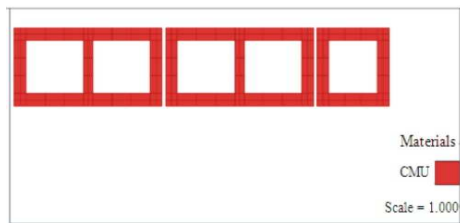


Fig. 2: Concrete masonry course consisting of full and half units

In order to overcome the problem of using a single analysis time step for the entire grid, the continuum grid was divided into computational partitions (zones) each with its own time step. The concrete masonry wall model before the application of the composite retrofit was shown in Fig. 3. The front view of the wall with composites and supporting boundary conditions was shown in Fig. 4.

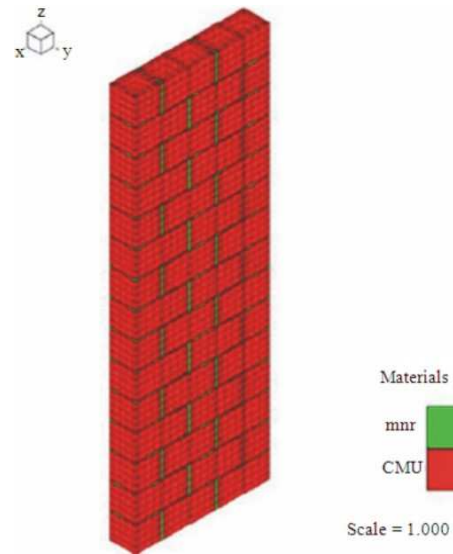


Fig. 3: Concrete masonry wall before applying composite retrofits

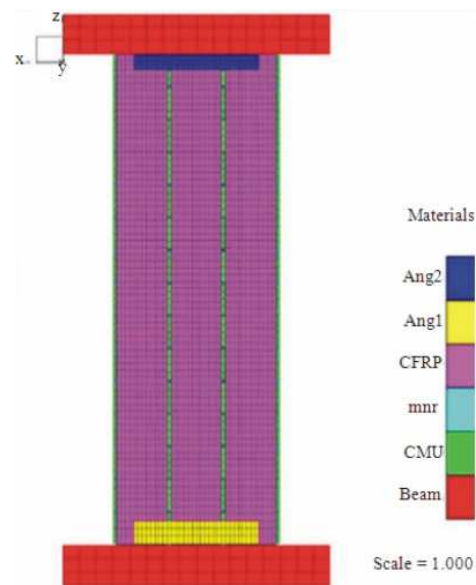


Fig. 4: Concrete masonry wall with composites and supporting boundary conditions

**RESULTS AND DISCUSSION**

In order to calculate loads, the stand-off distance of an explosive to each node of the model was of interest. The analysis presented in the first model run (also called original model in this study) assumes a spherical explosive charge with non-uniform pressure distribution for loading computations. The distance to each node was calculated from geometry assuming the explosive hits the wall at mid-height. The stand-off distance contour plot was determined from an array named “pldt\_max>1” as shown in Fig. 5 representing the distance of each node to the explosive charge. A geometry check near the roof the concrete masonry wall proved the validity of the outward normal contours from the explosion source shown in Eq. 5:

$$\text{Max. range} = \sqrt{R^2 + (h / 2)^2} \tag{5}$$

Where:

R = The stand-off distance

h = The wall height:

$$\text{Max. range} = \sqrt{1.83^2 + (3.05 / 2)^2} = 2.38 \text{ m (7.82 ft)}$$

The stand-off distance was then used to calculate pressure distribution based on air blast theory<sup>[2]</sup>. The corresponding pressure distribution contour was determined from an array named “pldt\_max>2” shown in Fig. 6. Similarly, a check was performed for the ratio of the peak pressures at mid-height to the peak pressure at the supporting floor using the Hopkinson-Cranz scaling law which predicts a cubic stand-off ratio of

$$\left( \frac{\sqrt{R^2 + (h / 2)^2}}{R} \right)^3$$

The ratio of the maximum to minimum pressure ratio was given in Eq. 6:

$$\frac{P_{\text{max}}}{P_{\text{min}}} = \left( 1 + \left( \frac{h}{2R} \right)^2 \right)^{3/2} \tag{6}$$

$$\frac{P_{\text{max}}}{P_{\text{min}}} = \left( 1 + \left( \frac{3.05}{2 \times 1.83} \right)^2 \right)^{3/2} = 2.2$$

The above result is in close agreement with the theoretical ratio  $\frac{91.8}{44} = 2.1$  of obtained from Fig. 6.

After the load on the wall is computed, the model was divided into five computational partitions (zones) with a calculated automatic model time steps of

0.00029 m sec for stability criteria. Two models were run: the first model for a wall hardened with two layers of composite and the second model with four layers of composite. Each model took 14.8 h to run on an AMD opteron dual processor in order to capture a displacement-time history response for 100 m sec. An example plot of maximum displacement contour profile at the end of the run for the two-layered composite wall was shown in Fig. 7. A post-processing of the model was conducted to extract displacement-time histories in an ASCII text file. The results were combined and plotted for both the two and four-layered composite hardened walls as shown in Fig. 8.

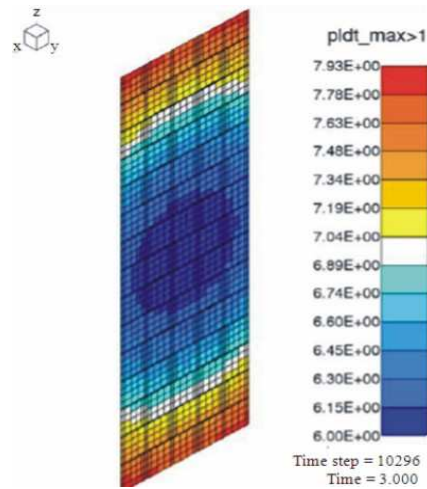


Fig. 5: Range from explosion to elements in feet (1 ft = 0.305 m)

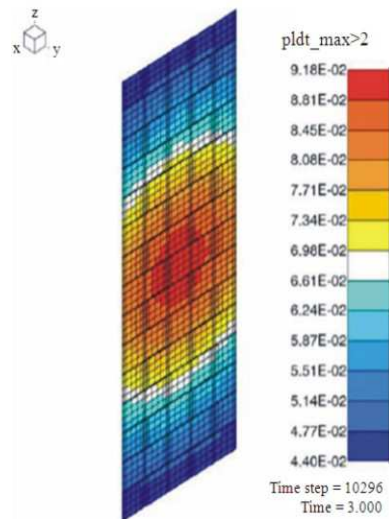


Fig. 6: Non-uniform pressure distribution in ksi (1 ksi = 6.90 MPa)

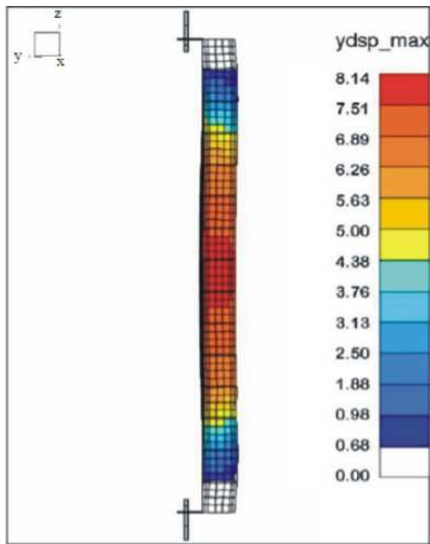


Fig. 7: Maximum displacement contour in inch (1 in = 2.54 cm)

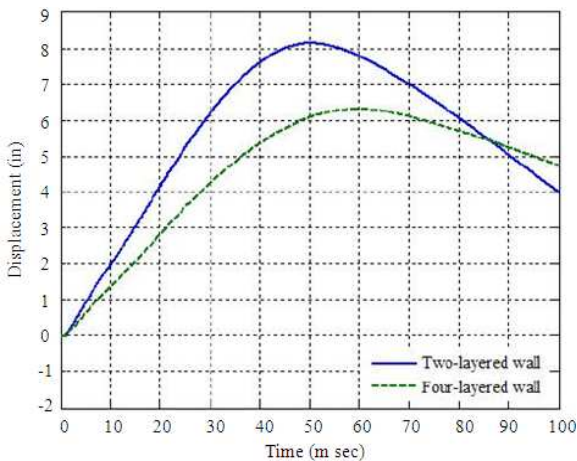


Fig. 8: Finite element predicted displacement-time histories (1 in = 2.54 cm)

The finite element analysis was able to predict large horizontal crack formation in the masonry at the mortar joints between the first and second course as shown in Fig. 9 (“evbr” is an array indicating plastic volumetric strain in percentage). This phenomenon was observed in a full-scale blast test<sup>[12]</sup>.

There were several uncertainties in the study of the response of concrete masonry walls retrofitted with composites and subjected to blast loading. Some of the uncertainties include pressure distribution assumptions in calculating wall loadings, effect of mid-height explosive bursts versus near the ground explosive burst, variations in modulus of elasticity of the concrete masonry,

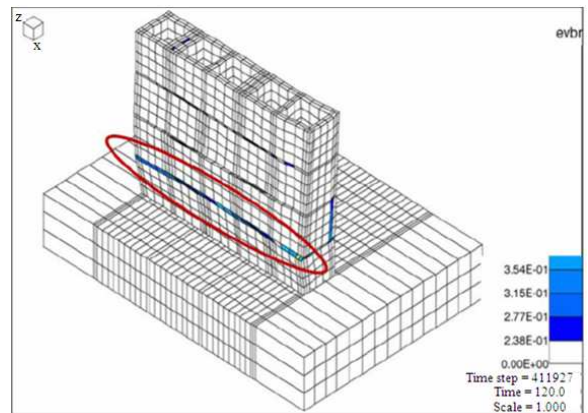


Fig. 9: Horizontal crack at the first course

securing mechanisms of the composite in insuring effectiveness during an explosion and selecting appropriate equations of state for shock progression. The developed finite element was used as a basis in investigating the changes in displacement-time history due to possible changes in input parameters. Due to computer resource limitation, the study was only focused on concrete masonry walls retrofitted with two layers of composites. The following changes in input parameters were investigated:

**Pressure distribution:** When an explosion from a high explosive source occurs within a structure, blast waves will be reflected from the inner surfaces of the structure and imploded towards the center. The amplitude of the re-reflected waves will decay with each reflection and eventually the pressure will settle to an ambient pressure. Some approaches in blast resistant design and analysis utilize a uniformly distributed peak reflected overpressures in order to simplify computational effort<sup>[1]</sup>. Hence, it will be beneficial to study the effect of a uniform blast pressure assumption on displacement-time history results as compared to the non-uniform blast distribution shown in Fig. 6.

In the original calculation (Fig. 6) the load was applied to the walls with an air blast in which the pressure varies from element to element. The pressure applied was stored in a data array containing a range of the element and the corresponding pressure value. In order to apply a uniform pressure, the range and the explosive incidence angle were explicitly set so that all surfaces were loaded with the same value of pressure.

The maximum uniform pressure was obtained when an outward normal from the loaded surface and a vector to the explosion were parallel (corresponding to an incidence angle of zero). A uniform pressure of 634 kPa (92 psi) was applied to the entire surface as shown

in Fig. 10. The model was run keeping all other parameters the same as the original model and the resulting displacement-time history comparison was shown in Fig. 11.

The uniform pressure assumption predicted a maximum displacement of 24.9 cm (9.8 in) as compared to a 20.6 cm (8.1 in) peak displacement for the non-uniform distribution. As expected, the uniform pressure distribution assumption resulted in increased

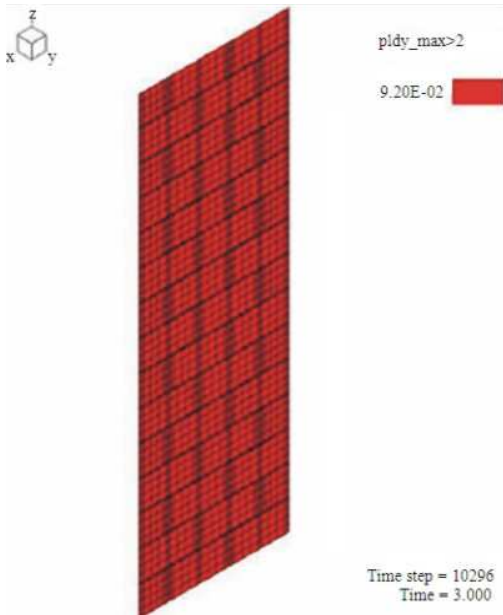


Fig. 10: Uniform pressure distribution in ksi (1 ksi = 6.90 MPa)

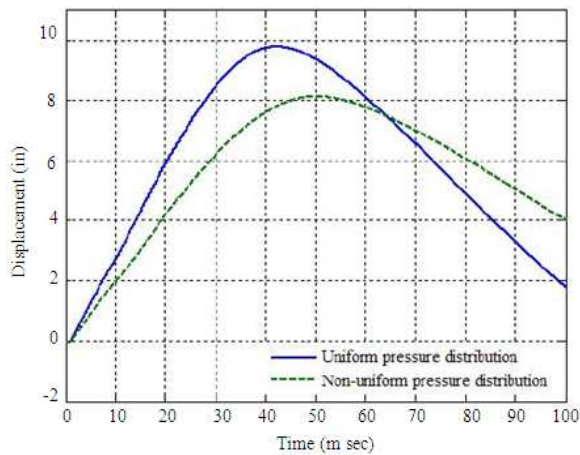


Fig. 11: Displacement-time history comparisons for variation in pressure distributions (1 in = 2.54 cm)

peak displacement value. The increase in peak displacement prediction is deemed acceptable from the design perspective because a higher peak displacement value will require more number of composites to harden a wall than a lower peak displacement value.

**Height of burst:** If a blast source is placed on or near the ground, then the initial shock is very quickly reflected. The reflected wave will merge with the incident wave so rapidly that a single, strengthened blast wave will be formed. The characteristic of this single wave is often almost identical with the characteristic of free-field explosions except that the blast source appears to have a greater energy.

Although the original model was subjected to a mid-height burst, there was an interest in investigating how the results (pressure distribution and displacement-time histories) would change if the explosive was on the ground. In order to achieve that comparison, a hemispherical shape explosive was used instead of spherical shape explosive charge. The range (distance) to the explosion due to the hemispherical blast was shown in Fig. 12 with the corresponding pressure distribution of Fig. 13. It was clear that the wall near the ground floor (the bottom side) was experiencing most of the pressure because of proximity to the explosive charge. The roof was subject to near zero pressure as it had the longest range to the explosion.

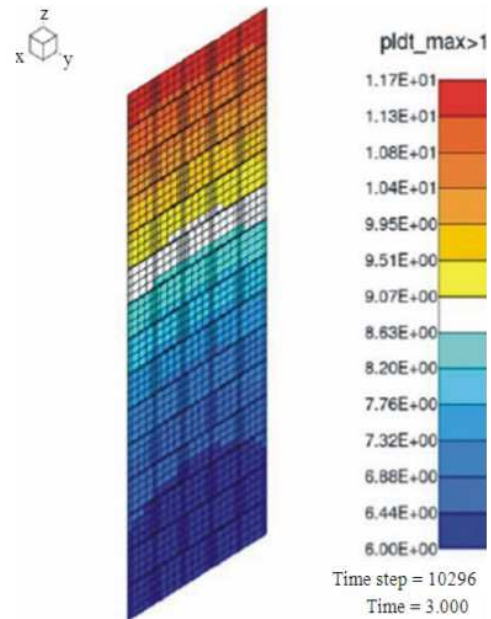


Fig. 12: Range from explosion to elements in feet (1 ft = 0.305 m)

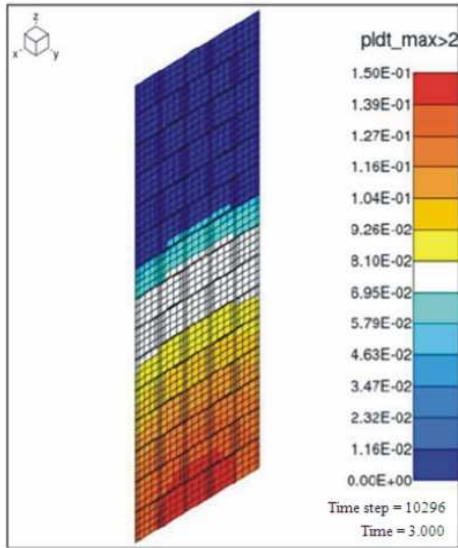


Fig. 13: Non-uniform pressure distribution in ksi (1 ksi = 6.90 MPa)

In the spherical explosive charge case (Fig. 6), the peak pressure was 0.633 MPa (91.8 psi). In the hemispherical explosive charge case (Fig. 13), the peak pressure was 1.03 MPa (150 psi). The proportion of energy reflected from the ground compared to the original model was estimated by comparing the peak pressure values which amounts to an increase of  $\frac{(1.03 - 0.633)}{0.633} = 62.7\%$ .

Theoretically if the ground was a perfectly rigid surface, the equivalent energy of the air blast wave would have been doubled (a 100% increase in energy). The model was run keeping all other parameters the same as the original model and the resulting displacement-time history comparison was shown in Fig. 14. A ground burst assumption predicted a peak displacement value of 26.2 cm (10.3 in), an increase of 27% when compared to the mid-height explosion peak displacement. The result indicates that explosive retrofit designs should account for the possibility of increased deflection (as a result of increased pressure) in determining the number of composite to harden a wall.

**Modulus of elasticity of the concrete masonry:** All the analysis presented thus far was based on a typical value of modulus of elasticity concrete masonry walls,  $E_m$ , of 10.4 GPa ( $1.5 \times 10^6$  psi) and a compressive strength,  $f_m$ , of 13.8 MPa (2000 psi). A parametric study was conducted in order to address how the results would change for different concrete masonry walls (different values of modulus of elasticity).

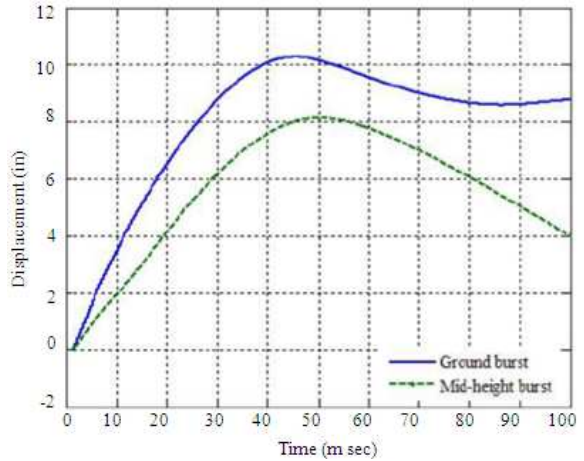


Fig. 14: Displacement-time comparisons for variations in height of burst (1 in = 2.54 cm)

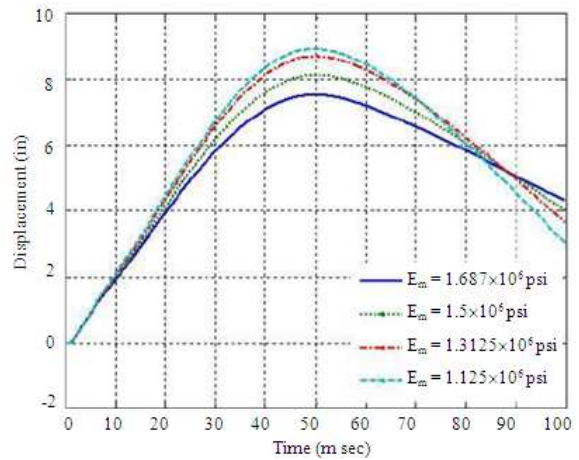


Fig. 15: Displacement-time comparisons for variations in the modulus of elasticity of concrete masonry (1 in = 2.54 cm)

The changes were made in the input file by varying the compressive strength of masonry and calculating the modulus of elasticity based on the recommendations of The Masonry Society as shown in Eq. 7<sup>[10]</sup>:

$$E_m = 750f_m \quad (7)$$

The model was run keeping all other parameters the same as the original model and the resulting displacement-time history comparison was shown in Fig. 15. The result showed that the compressive strength of the concrete masonry has small effect on the peak displacement values. The peak displacement values were summarized in Table 2. The Table 2 shows

Table 2: Peak displacement comparisons

Masonry strength MPa (psi)	Modulus of elasticity GPa (psi)	Peak displacement cm (in)
10.3 (1500)	7.76 (1.125×10 <sup>6</sup> )	22.6 (8.9)
12.1 (1750)	9.05 (1.3125×10 <sup>6</sup> )	22.1 (8.7)
13.8 (2000)	10.30 (1.5×10 <sup>6</sup> )	20.6 (8.1)
15.5 (2250)	11.60 (1.6875×10 <sup>6</sup> )	19.3 (7.6)

that the difference in peak displacement value is only 3.3 cm (1.3 in) for the lower and higher strengths of concrete masonry. This fact is supported by observation of failure mechanism in full-scale field tests<sup>[9]</sup>. The inability of the concrete masonry to contribute to the structural stiffness during blast and the ability of the composite to withstand the blast pressure through large nonlinear deformation is the basis for developing retrofit design guidelines.

### CONCLUSION

Finite element analysis of concrete masonry walls retrofitted with composites and subjected to blast load was presented. Displacement-time history responses were studied which form the basis for continuing work on retrofit design guidelines for blast loadings. Parametric variation in material properties and loadings were investigated. Uniformly distributed blast loads over a wall height produced a small difference in peak displacement results when compared to the non-uniform pressure distribution. Ground explosive burst was shown to produce a 62.7% increase in energy and a higher peak displacement response when compared to mid-height explosive burst. The parametric study on the variation of modulus of elasticity of concrete masonry showed no significant effect on peak displacement affirming the use of the resistance deflection contribution of the composite in retrofit designs.

### ACKNOWLEDGEMENT

The researcher gratefully acknowledges the support of Darren Tennant (Principal, Weidlinger Associates Inc.).

### REFERENCES

1. American Society of Civil Engineers, 1997. Design of blast resistant buildings in petrochemical facilities. New York.
2. Baker, W.E., 1973. Explosions in Air. University of Texas Press, Austin, TX., ISBN :10: 0292720033, pp: 285.

3. Belytschko, T., W.K. Liu and B. Moran, 2000. Nonlinear Finite Elements for Continua and Structures. John Wiley and Sons Ltd., England, ISBN: 978-0-471-98774-1, pp: 666.
4. Conrath, E.J., 1999. Structural Design for Physical Security: State of the Practice. ASCE Publication, American Society of Civil Engineers, Reston, VA., ISBN: 0784404577, pp: 264.
5. Cook, R.D., D.S. Malkus, M.E. Plesha and R.J. Witt, 2001. Concepts and Applications of Finite Element Analysis. 4th Edn., John Wiley and Sons Inc., New York, ISBN: 10: 0471356050, pp: 784.
6. Dennis, S.T., J.T. Baylot and S.C. Woodson, 2002. Response of ¼-scale concrete masonry unit walls to blast. J. Eng. Mech., 128: 134-142. DOI: 10.1061/(ASCE)0733-9399(2002)128:2(134)
7. Eamon, C.D., J.T. Baylot and J.L. O'Daniel, 2004. Modeling concrete masonry walls subjected to explosive loads. J. Eng. Mech. Facil., 130: 1098-1106.
8. Hetherington, J.G. and P.D. Smith, 1994. Blast and Ballistic Loading of Structures. Laxton's Oxford, UK., ISBN: 10: 0750620242, pp: 336.
9. Maji, A.K., J.P. Brown and G.S. Urgessa, 2008. Full-scale testing and analysis for blast-resistant design. J. Aerosp. Eng., 21: 217-225. DOI: 10.1061/(ASCE)0893-1321(2008)21:4(217)
10. Masonry Standards Joint Committee, 1999. Building Code Requirements for Masonry Structures. American Concrete Institute, Detroit, MI., ISBN: 1929081022, pp: 147.
11. Smilowitz, R. and M. Ettouney, 2000. Hazard reduction in structures subjected to explosive threats. J. Technol., 55-64. <http://direct.bl.uk/bld/PlaceOrder.do?UIN=072714076&ETOC=RN&from=searchengine>
12. Urgessa, G. and A. Maji, 2006. Blast response of carbon-fiber reinforced masonry walls. Proceeding of the 23th Conference on Theoretical and Applied Mechanics, May 2006, Society for Experimental Mechanics, Mayaguez, Puerto Rico.
13. Vaughan, D.K., 2005. Flex User's Manual Version 1-J.9. Weidlinger Associates Inc., Los Altos, CA.
14. Ward, S.P., 2004. Retrofitting existing masonry buildings to resist explosions. J. Perform. Constr. Facil., 18: 95-99.
15. Zukas, J.A., 2004. Introduction to Hydrocodes. Elsevier Ltd., Oxford, UK., ISBN: 10: 0080443486, pp: 326.